PtdIns(4,5)P_2 turnover is required for multiple stages during clathrin- and actin-dependent endocytic internalization

Yidi Sun, Susheela Carroll, Marko Kaksonen, Junko Y. Toshima, and David G. Drubin

Department of Molecular and Cell Biology, University of California, Berkeley, Berkeley, CA 94720

The lipid phosphatidylinositol-4,5-bisphosphate (PtdIns[4,5]P_2) appears to play an important role in endocytosis. However, the timing of its formation and turnover, and its specific functions at different stages during endocytic internalization, have not been established. In this study, Sla2 ANTH-GFP and Sjl2-3GFP were expressed as functional fusion proteins at endogenous levels to quantitatively explore PtdIns(4,5)P_2 dynamics during endocytosis in yeast. Our results indicate that PtdIns(4,5)P_2 levels increase and decline in conjunction with coat and actin assembly and disassembly, respectively. Live-cell image analysis of endocytic protein dynamics in an *sjl1Δ sjl2Δ* mutant, which has elevated PtdIns(4,5)P_2 levels, revealed that the endocytic machinery is still able to assemble and disassemble dynamically, albeit nonproductively. The defects in the dynamic behavior of the various endocytic proteins in this double mutant suggest that PtdIns(4,5)P_2 turnover is required for multiple stages during endocytic vesicle formation. Furthermore, our results indicate that PtdIns(4,5)P_2 turnover may act in coordination with the Ark1/Prk1 protein kinases in stimulating disassembly of the endocytic machinery.

Introduction

Several lines of evidence have implicated the minor phospholipid phosphatidylinositol-4,5-bisphosphate (PtdIns[4,5]P_2) as a key regulator of clathrin- and actin-dependent endocytosis. First, PtdIns(4,5)P_2-binding domains are present in many endocytic proteins, including AP-2, Hip1R/Sla2p, epsin/Ent1p/Ent2p, AP180/YAP180, amphiphysin/Rvs161/167, and dynamin, and abrogating the PtdIns(4,5)P_2 binding ability of these proteins impairs endocytosis (Jost et al., 1998; Gaidarov and Keen, 1999; Takei et al., 1999; Vallis et al., 1999; Ford et al., 2001; Itoh et al., 2001; Sun et al., 2005; Friesen et al., 2006). Second, several phosphoinositide kinases and phosphatases, which are involved in controlling the production and elimination of PtdIns(4,5)P_2, physically interact with endocytic proteins (McPherson et al., 1996; Haffner et al., 1997; Padron et al., 2003; Stefan et al., 2005; Bairstow et al., 2006), and mutations in these enzymes often lead to altered PtdIns(4,5)P_2 levels and endocytic defects (Singer-Kruger et al., 1998; Cremona et al., 1999; Di Paolo et al., 2004). Third, PtdIns(4,5)P_2 has been implicated in actin assembly (Yin and Janmey, 2003), which is important for endocytosis in many cell types.

Although these various observations suggest that modulation of PtdIns(4,5)P_2 levels is integral to coordination of endocytic events, little is known about how PtdIns(4,5)P_2 levels at endocytic sites change as a function of time, and how such changes might affect the functions of endocytic proteins at different steps of endocytic internalization.

In the past several years, quantitative analysis of endocytic protein dynamics using multicolor real-time fluorescence microscopy and particle tracking algorithms has greatly contributed to our knowledge of the endocytic internalization process (Merrifield, 2004). To extend this type of analysis to PtdIns(4,5)P_2 dynamics during endocytic internalization, probes that bind to PtdIns(4,5)P_2 specifically at endocytic sites are necessary. Evidence for PtdIns(4,5)P_2 enrichment at endocytic sites has not been obtained. GFP-tagged PLCδ-PH, which binds to PtdIns(4,5)P_2 with high specificity in vitro (Lemmon et al., 1995), has been widely used in studying PtdIns(4,5)P_2 localization in live cells. However, when expressed in yeast at high levels, GFP-2xPLCδ-PH from rat labeled the yeast plasma membrane uniformly instead of showing the patchlike localization that characterizes endocytic proteins (Stefan et al., 2002). Recent studies identified a new PtdIns(4,5)P_2 binding domain,

Correspondence to David G. Drubin: drubin@berkeley.edu

Abbreviations used in this paper: ANTH, AP180 N-terminal homology; Clc, clathrin light chain; PH, pleckstrin homology; PtdIns(4,5)P_2, phosphatidylinositol-4,5-bisphosphate.

The online version of this article contains supplemental material.

The Journal of Cell Biology, Vol. 177, No. 2, April 23, 2007 355–367
http://www.jcb.org/cgi/doi/10.1083/jcb.200611011

the AP180 N-terminal homology (ANTH) domain (Ford et al., 2001; Itoh et al., 2001). Interestingly, most ANTH domain–containing proteins are involved in endocytosis. Thus, it is possible that an ANTH domain could detect PtdIns(4,5)P_2 at endocytic sites, especially if it is expressed at endogenous levels. Although PtdIns(4,5)P_2-binding domains have so far not been localized specifically to endocytic sites, synaptojanins, which are inositol-polyphosphate 5-phosphatases, have been detected at clathrin-coated endocytic intermediates at nerve terminals and at endocytic sites in yeast cells (McPherson et al., 1996; Haffner et al., 1997; Cremona et al., 1999; Stefan et al., 2005). Therefore, high time resolution live-cell imaging of synaptojanin proteins could predict when PtdIns(4,5)P_2 levels change in vivo. Because overexpression of inositol-polyphosphate 5-phosphatases is expected to change PtdIns(4,5)P_2 levels, it is critical to perform this type of analysis on synaptojanin expressed at endogenous levels. However, because the fluorescence signal of endogenous synaptojanin proteins is often difficult to detect, quantitative analysis of endogenous synaptojanin protein dynamics has not yet been done.

A mutant defective in synaptojanin function, *sjl1Δ sjl2Δ*, provides the ability to test PtdIns(4,5)P_2 functions at endocytic sites. Previous studies demonstrated that cellular PtdIns(4,5)P_2 levels in *sjl1Δ sjl2Δ* cells are two- to threefold higher than in wild-type cells (Stolz et al., 1998). *sjl1Δ sjl2Δ* cells also show a severe defect in both receptor-mediated and fluid-phase endocytosis (Singer-Kruger et al., 1998). Moreover, this mutant exhibits abnormal deep invaginations of the plasma membrane proposed to be generated by the formation of an endocytic bud, which cannot undergo fission (Singer-Kruger et al., 1998; Stefan et al., 2005). However, the dynamics of endocytic proteins associated with these abnormal membrane structures has not been explored.

In this study, we used two functional GFP-tagged protein probes, Sla2 ANTH-GFP and Sjl2-3GFP, expressed at endogenous levels to quantitatively analyze the dynamic turnover of PtdIns(4,5)P_2 during endocytic internalization in live cells. Furthermore, we also investigated how PtdIns(4,5)P_2 turnover affects different stages of endocytic vesicle formation by examining dynamics of various GFP-tagged endocytic proteins in synaptojanin mutants.

Results

Visualizing PtdIns(4,5)P_2 at endocytic sites using a GFP-fused ANTH domain

To detect PtdIns(4,5)P_2 at endocytic sites in vivo, we first needed to develop and validate a probe. Sla2p is an essential protein for yeast endocytosis that contains an ANTH domain, a coiled-coil domain, and a talin-like domain (Wesp et al., 1997; Ford et al., 2001; Itoh et al., 2001; Sun et al., 2005). Previously, we showed that Sla2p binds through its ANTH domain to PtdIns(4,5)P_2 specifically (Sun et al., 2005). We fused GFP to the C terminus of the first 360 aa of Sla2p, which includes the ANTH domain but not the central coiled-coil domain or the talin-like domain. The wild-type *SLA2* gene was replaced with this construct so

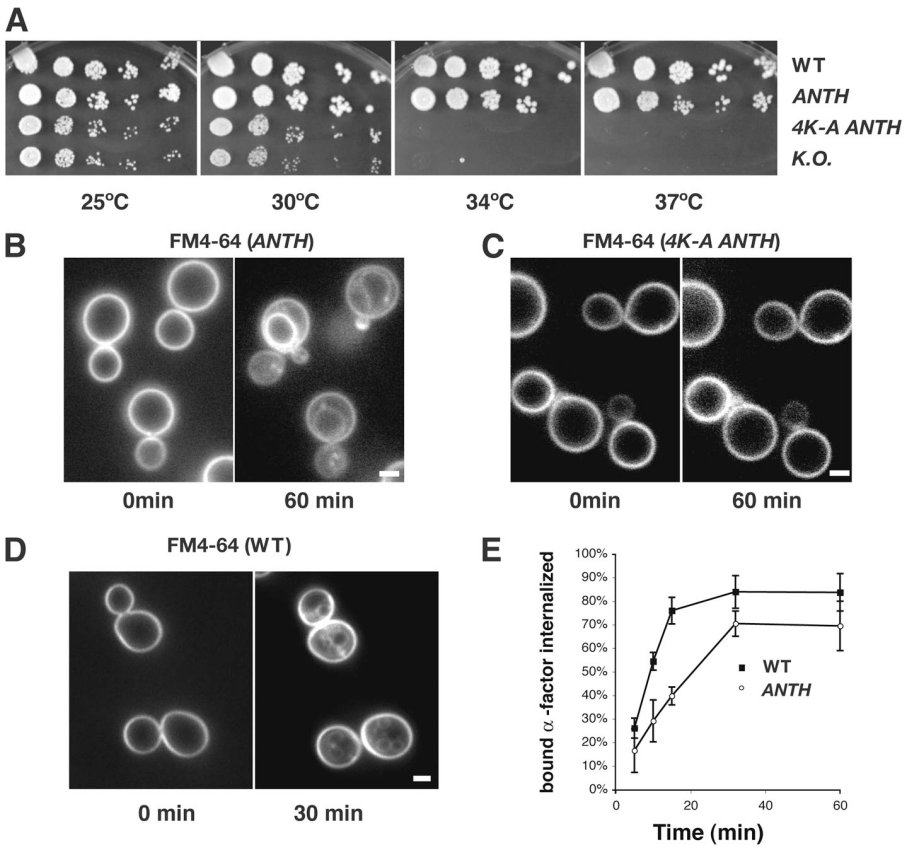

Figure 1. **Sla2 ANTH-GFP is at least partially functional in endocytic internalization.** (A) Growth of *sla2* mutants. Strains were grown on YPD plates at the indicated temperatures. (B–D) FM4-64 uptake assay. Cells were treated with media containing FM4-64 in a flow chamber. FM4-64 was visualized by fluorescence microscopy every 10 min. Pictures were taken at 0 and 30 or 60 min (E) Receptor-mediated internalization of [^{35}S]methionine-labeled α-factor in wild-type cells and *sla2ANTH-GFP* mutants after a 5-min preincubation at 25°C. Error bars represent the SD from three experiments. Bars, 2 μm.

that ANTH-GFP would be expressed from the *SLA2* promoter. We will refer to the resulting strain as *sla2 ANTH-GFP*. As a control, we also generated a *sla2 4K-A ANTH*-GFP mutant, in which four lysine residues of Sla2 ANTH required for PtdIns(4,5)P_2 binding in vitro were changed to alanine (Sun et al., 2005). Sla2 ANTH-GFP and Sla2 4K-A ANTH-GFP expression levels were shown to be similar by using antibodies against Sla2p or against GFP on immunoblots of cell extracts (unpublished data). Although *sla2Δ* strains are temperature sensitive (Wesp et al., 1997), *sla2 ANTH-GFP* exhibited normal growth at 37°C (Fig. 1 A). In addition, although endocytosis is completely inhibited in *sla2Δ* cells (Wesp et al., 1997), the endocytic membrane marker FM4-64 was internalized to the vacuole membrane in *sla2 ANTH-GFP* cells, albeit in 60 min (Fig. 1 B), which is slower than in wild-type cells (Fig. 1 D; Vida and Emr, 1995). We also examined the internalization rate of *sla2 ANTH-GFP* cells using the [^{35}S]methionine-labeled α-factor uptake assay. As shown in Fig. 1 E, the α-factor uptake rate for the *sla2 ANTH-GFP* strain was about half that of wild-type cells (Fig. 1 E). These results demonstrate that Sla2 ANTH-GFP is able to at least partially perform Sla2p's function in endocytic internalization.

Previously, we showed that wild-type Sla2-GFP colocalizes with and exhibits similar dynamic behavior to the endocytic coat protein marker, Sla1p (Kaksonen et al., 2003). Both Sla2p and Sla1p form cortical patches at the plasma membrane, and then move off the cortex toward the cell center, which likely represents membrane invagination. Interestingly, Sla2 ANTH-GFP showed patchlike localization on the plasma membrane, whereas Sla2 4K-A ANTH-GFP was only detected in the cytoplasm (Fig. 2 A and Video 1, available at http://www.jcb.org/cgi/content/full/jcb.200611011/DC1), indicating that the interaction of the ANTH domain with PtdIns(4,5)P_2 is crucial for the patchlike localization. The lifetime of Sla2 ANTH-GFP patches was 105 ± 28.7 s, which is ~3 times longer than the lifetime of wild-type Sla2-GFP patches (36.6 ± 6.4 s). The longer lifetime of Sla2 ANTH-GFP patches is consistent with the reduced rate of endocytosis observed in this mutant. Furthermore, compared with Sla2-GFP, more Sla2 ANTH-GFP was observed in the cytoplasm, which is probably because the coiled-coil domain binds to other endocytic proteins, and the talin-like domain binds to F-actin (McCann and Craig, 1997; Henry et al., 2002; Gourlay et al., 2003). These interactions may enhance the recruitment of full-length Sla2p to endocytic sites. *sla2 4K-A ANTH-GFP* cells, in which Sla2 4K-A ANTH-GFP does not localize to the cell cortex, showed a growth defect and complete endocytosis defect that was characteristic of *sla2Δ* cells (Fig. 1, A and C; Wesp et al., 1997). Together, these data indicate that the Sla2 ANTH-GFP is sufficient for localization at the cell cortex, and that this localization is dependent on PtdIns(4,5)P_2 binding.

To confirm that Sla2 ANTH-GFP patches correspond to endocytic sites, we performed two-color real-time microscopy. Most clathrin light chain 1 (Clc1)-GFP patches on the cell cortex colocalized with ANTH-mCherry (Fig. 2 B).

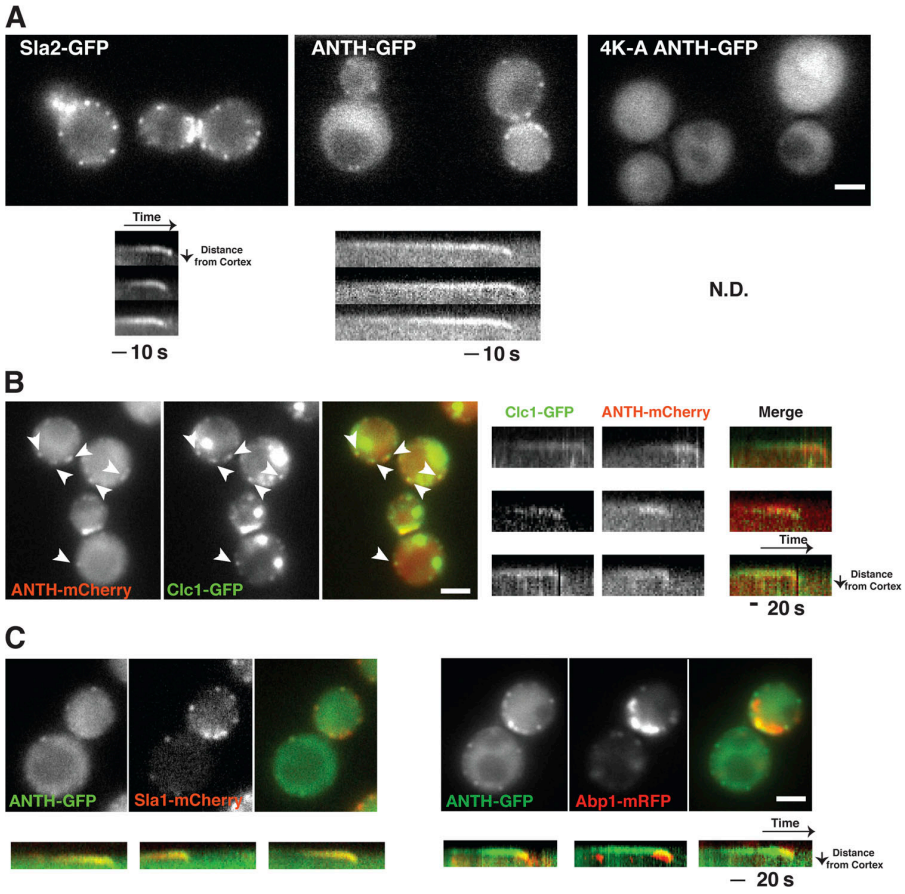

Figure 2. **Sla2 ANTH-GFP dynamics at endocytic sites.** (A) Single frames from videos of live cells expressing different GFP-tagged proteins (top). Kymographs of single patches from videos of cells expressing the indicated GFP-tagged protein (1 frame/s; bottom). (B) Simultaneous localization of Clc1-GFP and Sla2-ANTH-mCherry in live cells. Kymographs of individual patches from 2-color videos of cells expressing Clc1-GFP and Sla2-ANTH-mCherry. (C) Simultaneous localization of GFP- and RFP-tagged proteins in live cells (top). Kymographs of individual patches from 2-color videos of cells expressing Sla2-ANTH-GFP and Sla1-mCherry, or Sla2-ANTH-GFP and Abp1-RFP (bottom). Bars, 2 μm.

Kymographs revealed that ANTH-mCherry joins the patches shortly after cortical Clc1-GFP appears in the patches (Fig. 2 B). As shown in Fig. 2 C, Sla2 ANTH-GFP and the endocytic coat protein marker Sla1-mCherry accumulate at the cell cortex with similar timing (Fig. 2 C and Video 2, available at http://www.jcb.org/cgi/content/full/jcb.200611011/DC1), and then make an inward movement together when the cortical actin marker Abp1p joins the patch (Fig. 2 C and Video 3). The yeast cortical actin patches are endocytic sites, and the inward movement of the endocytic coat represents membrane invagination (Kaksonen et al., 2003). These results suggest that Sla2 ANTH-GFP serves as a valid PtdIns(4,5)P_2 marker at endocytic sites in vivo. Furthermore, the synchronous dynamics of the Sla2 ANTH-GFP and Sla1-mCherry provide support for the idea that endocytic coat protein recruitment and subsequent disappearance at endocytic sites are, at least in part, the result of changes in PtdIns(4,5)P_2 levels.

Monitoring PtdIns(4,5)P_2 dynamics during endocytic internalization using Sjl2-3GFP

To further examine PtdIns(4,5)P_2 dynamics during endocytic internalization in wild-type cells, we tagged with GFP a phosphoinositide kinase and two phosphoinositide phosphatases, which control PtdIns(4,5)P_2 levels and have been implicated in endocytosis (Singer-Kruger et al., 1998; Stolz et al., 1998; Desrivieres et al., 2002). The GFP-tagged proteins were expressed from the endogenous promoters of the respective genes. Genetic studies confirmed that these GFP-tagged enzymes are functional (Fig. S1 A). The motivation for these studies was to monitor the dynamics of these enzymes at high temporal and spatial resolution to predict how local PtdIns(4,5)P_2 concentration changes may relate the specific steps in endocytic internalization. Mss4p is the only phosphatidylinositol-4-phosphate 5-kinase expressed in budding yeast (Desrivieres et al., 1998; Homma et al., 1998). Mss4-GFP was observed both in the cytoplasm and at the cell cortex (Fig. S1 B). Although Mss4-GFP showed a patch pattern at the plasma membrane, it was not polarized like endocytic proteins. Moreover, colocalization between Mss4-GFP and endocytic coat marker proteins, such as Ede1p and Sla1p, was not apparent (unpublished data). These results suggest that PtdIns(4,5)P_2 may not be selectively synthesized at sites of endocytosis.

The yeast synaptojanins Sjl1p and Sjl2p, which are inositol-polyphosphate 5-phosphatases, have previously been implicated in endocytosis (Singer-Kruger et al., 1998). Although Sjl1-GFP mostly localized to the cytoplasm (Fig. S1 D), Sjl2-GFP appeared in polarized patch structures at the cell cortex (Fig. S1 C). Interestingly, more cortical Sjl1-GFP was observed in an *sjl2Δ* strain (Fig. S1 E), which is consistent with the possibility that Sjl1p and Sjl2p may share functions. Based on these observations, Sjl2p appeared to be the most suitable probe for dynamic regulation of PtdIns(4,5)P_2 levels during endocytosis.

Overexpressed Sjl2$^{\Delta\text{-}37}$-GFP (lacking the final 37 Sjl2 amino acids) was previously shown to colocalize with Abp1-DsRed in live cells (Stefan et al., 2002). However, because DsRed is an obligate tetramer, actin dynamics may have been altered in those studies. Indeed, expression of Abp1-DsRed in our strain background caused abnormal actin patch dynamics (unpublished data). Abp1 tagged with GFP or monomeric RFP is a well-validated marker for endocytic actin structures (Kaksonen et al., 2003; Sun et al., 2006). Moreover, overexpression of Sjl2p may have altered PtdIns(4,5)P_2 levels or protein localization in the earlier study. To monitor Sjl2p dynamics quantitatively during different steps of endocytic internalization, expressing Sjl2p at endogenous levels is critical. We created a construct to fuse 3GFP to the Sjl2p C terminus, and expressed the fusion protein from the *SJL2* chromosomal locus (Fig. 3 A and Video 4, available at http://www.jcb.org/cgi/content/full/jcb.200611011/DC1). Phenotypic analysis confirmed that Sjl2-3GFP is functional (Fig. S1 A). Sjl2-3GFP appeared at cortical patches. The lifetime of Sjl2-3GFP patches was ~9.8 ± 1.4 s, which is shorter than the lifetime of the cortical actin marker Abp1 (14.7 ± 1.6 s). Sjl2-3GFP patches had an initial nonmotile phase, which was followed by a transition to a highly motile phase (Fig. 3 B). The fluorescence intensity of the Sjl2-3GFP patches developed in a very regular manner, reaching maximum

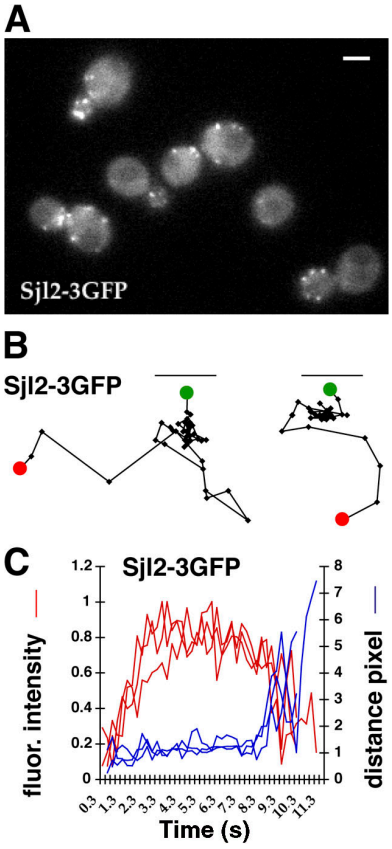

Figure 3. **Sjl2-3GFP dynamics at endocytic sites.** (A) Single frame from a video of live cells expressing 3GFP-tagged Sjl2p. Bar, 2 μm. (B) Tracking of individual Sjl2-3GFP patches. Positions of the centers of patches were determined in each frame of a video from a medial focal plane of a cell, and consecutive positions were connected by lines. Green and red dots denote the first and last positions, respectively, of each patch. Patch traces are oriented so that the cell surface is up and the cell interior is down. The time difference between each position along the track is 0.25 s. (C) Quantitation of fluorescence intensity and distance from the site of patch formation for Sjl2-3GFP–labeled patches as a function of time. Each curve represents data from one patch. Fluorescence intensity over time was corrected for photobleaching.

intensity in only ~3 s, indicating that Sjl2p is rapidly recruited to the cell cortex (Fig. 3 C). Sjl2-3GFP remained at its maximal level for ~5 s, and then its levels started to decrease as it moved off of the cell cortex.

We previously established analytical probes and methods for dissecting different steps of endocytic internalization in live cells (Kaksonen et al., 2003). Actin assembly (detected using Abp1-GFP) accompanies the slow inward movement of the endocytic coat (labeled by fluorescent Sla1p) off of the plasma membrane. The slow Sla1p movement, and the subsequent fast Abp1p movement, likely reflect membrane invagination and movement of the released endocytic vesicle, respectively (Fig. 4 D; Kaksonen et al., 2003). To determine the exact endocytic steps during which Sjl2p is associated with endocytic sites, we imaged Sjl2-3GFP and Abp1-RFP simultaneously with a high temporal resolution of 1 s (Video 5, available at http://www.jcb.org/cgi/content/full/jcb.200611011/DC1). As shown in Fig. 4 (A–C), Sjl2-3GFP appears 5–6 s after Abp1p, and they move rapidly away from plasma membrane together. Strikingly, alignment analysis showed that Sjl2p recruitment to endocytic sites starts only when both Sla1p and Abp1p intensities are close to their maximum levels (Fig. 4 D), suggesting that PtdIns(4,5)P_2 is only eliminated after endocytic coat and actin assembly have occurred. This result is in agreement with the possibility that PtdIns(4,5)P_2 plays a role in recruitment of the coat proteins and cytoskeleton proteins to endocytic sites. Sjl2p begins to accumulate ~5 s after Abp1p, but rapidly reaches its maximum level at about the same time as Abp1p (Fig. 4 D). Sla1p intensity decreases as Sjl2p levels rapidly rise, supporting a role in uncoating (Fig. 4 D). Sjl2p remains at its maximum level, whereas Abp1p intensity decreases, implicating Sjl2p in actin disassembly. Furthermore, Sjl2p remains at its maximum intensity until the Abp1p/Sjl2p fast movement starts, which occurs after vesicle scission and uncoating (Fig. 4 D). Together, the highly regular dynamics of Sjl2p at endocytic sites suggests that PtdIns(4,5)P_2 levels are strictly controlled temporally during endocytotic internalization.

Endocytic patch dynamics associated with the large, abnormal plasma membrane invaginations observed in *sjl1Δ sjl2Δ* mutants

We next tested the impact of altered PtdIns(4,5)P_2 levels on spatial and temporal aspects of endocytosis. To do this, we studied endocytic defects of a mutant in which PtdIns(4,5)P_2 cannot be properly broken down. Although a triple null mutant of all three yeast synaptojanin genes, *sjl1Δ sjl2Δ sjl3Δ*, is not viable, the *sjl1Δ sjl2Δ* double mutant is viable (Stolz et al., 1998). Previous studies demonstrated that cellular PtdIns(4,5)P_2 levels in *sjl1Δ sjl2Δ* cells are two- to threefold higher than in wild-type cells (Stolz et al., 1998). Thus, this mutant provides an opportunity to determine how misregulation of PtdIns(4,5)P_2 levels affects endocytosis.

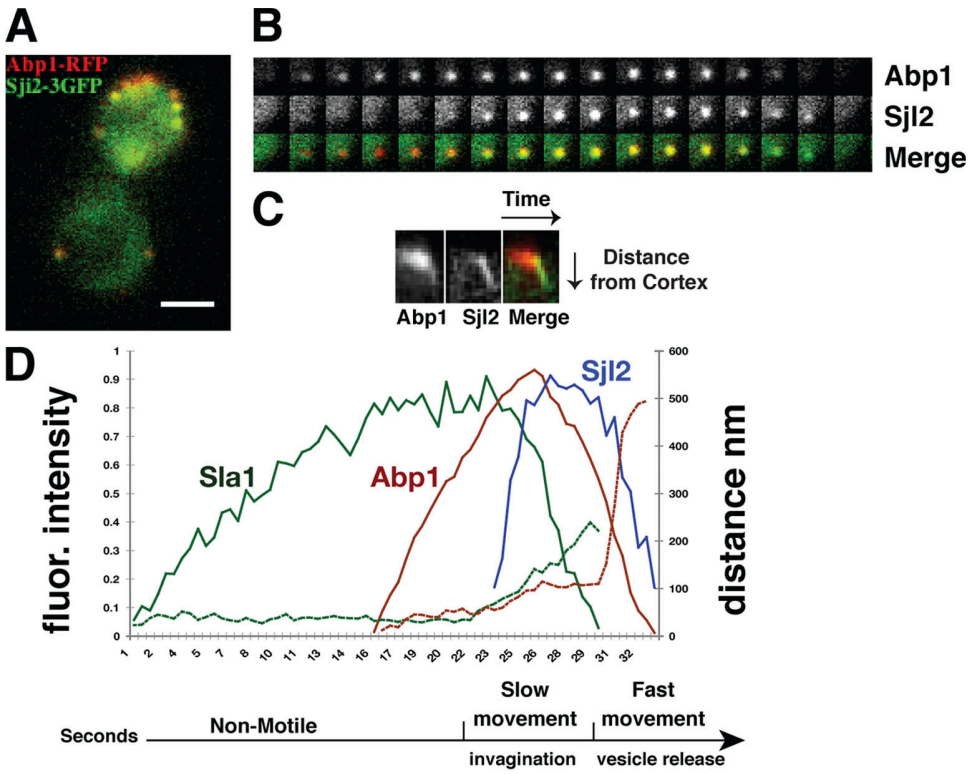

Figure 4. **Sjl2 dynamics during endocytic internalization.** (A) Single frame from video of yeast expressing Abp1-RFP (red) and Sjl2-3GFP (green). Bar, 2 μm. (B) Single-channel or merged image montages of single patches from two-color videos of cells expressing Abp1-RFP and Sjl2-3GFP. (C) Kymograph representation of Abp1-RFP and Sjl2-3GFP in a single patch over time. (D) Alignment of averaged patch intensity measurements of endocytic proteins. The data from at least three patches were averaged using one-color videos of GFP-tagged endocytic proteins. Data for Sla1p and Abp1p were aligned by time separating intensity peaks in two-color videos (Kaksonen et al., 2003). Abp1p and Sjl2p were aligned in reference to the time when the fast movement starts.

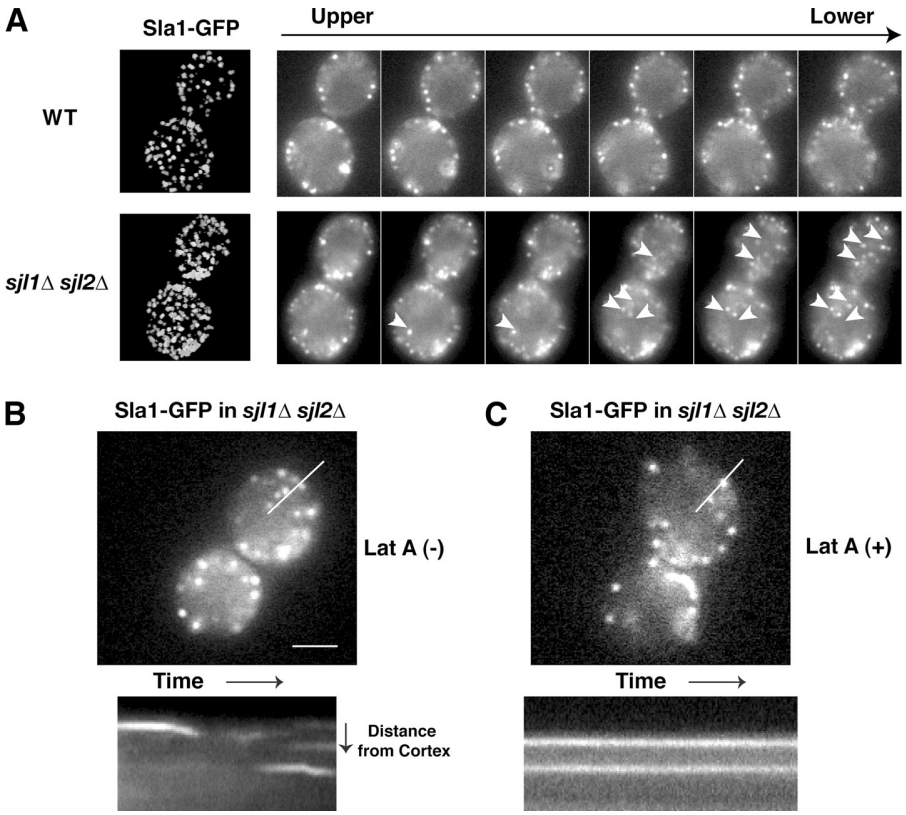

Figure 5. **Sla1-GFP localization in *sjl1Δ sjl2Δ* cells.** (A) Maximum intensity projection of z stacks for wild-type and *sjl1Δ sjl2Δ* cells expressing Sla1-GFP (left). Fluorescence intensity over time was corrected for photobleaching. Selected frames of z stack section around medial focal plane (right). Z axis interval is 300 nm. Arrows indicate the patches inside the cell. (B and C) *sjl1Δ sjl2Δ* cells expressing Sla1-GFP, and kymograph representation of Sla1-GFP patches on cortex and inside of the cell over time in the presence or absence of lat A. Bars, 2 μm.

In wild-type cells, the endocytic coat marker Sla1p arrives and disappears at patches with a lifetime 36.7 ± 8.5 s (Fig. 8 B; Kaksonen et al., 2003). However, in *sjl1Δ sjl2Δ* mutants, in addition to appearing on the cell cortex, Sla1-GFP patches were also observed inside the cells (Fig. 5 A). Both the internal and the cortical Sla1-GFP patches had similar lifetimes of 43.9 ± 5.8 s (Fig. 8 B). Quantification revealed a 51% increase in the number of Sla1p patches per cell surface area in *sjl1Δ*

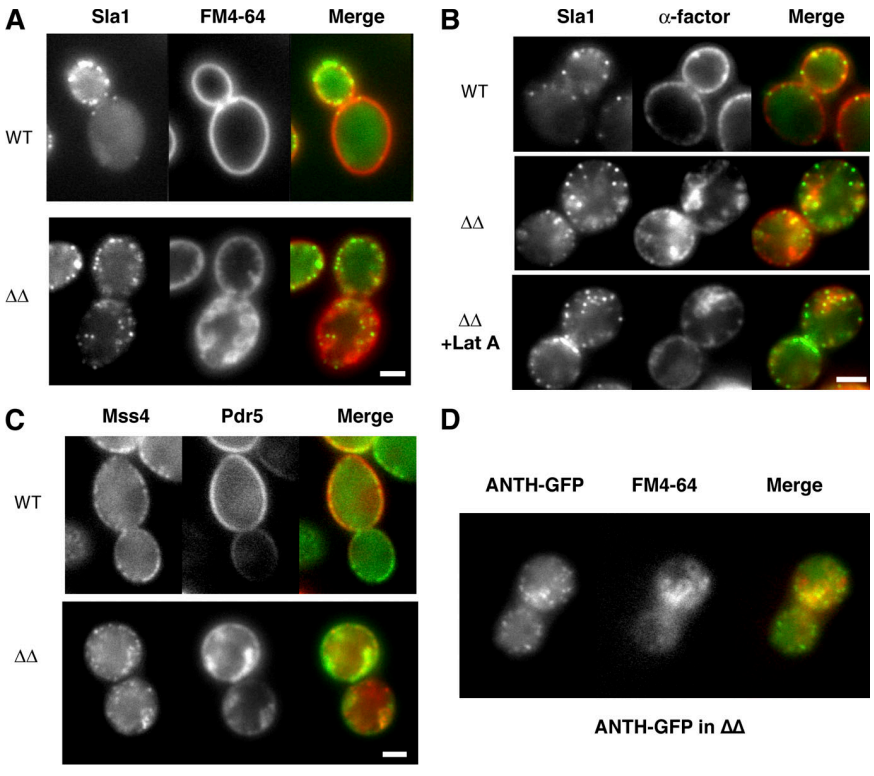

Figure 6. **Sla1p patches in the abnormal, deep membrane invaginations observed in the *sjl1Δ sjl2Δ* mutant.** (A) FM4-64 labeling of wild-type or *sjl1Δ sjl2Δ* cells expressing Sla1-GFP. FM4-64 and Sla1GFP were visualized immediately after FM4-64 was added to the media in a flow chamber. (B) Alexa Fluor 594–α-factor labeling of wild-type or *sjl1Δ sjl2Δ* cells expressing Sla1-GFP. Alexa Fluor 594–α-factor and Sla1p were visualized immediately after internalization was initiated in the presence or absence of lat A. (C) Wild-type or *sjl1Δ sjl2Δ* cells expressing Mss4-GFP and Pdr5-RFP. (D) FM4-64 labeling of *sjl1Δ sjl2Δ* cells expressing Sla2 ANTH-GFP. FM4-64 and Sla2 ANTH-GFP were visualized immediately after FM4-64 was added to the media in a flow chamber. Bars, 2 μm.

sjl2Δ mutants (Fig. 5 A). Furthermore, turnover of Sla1-GFP patches at both locations was blocked by addition of the actin assembly inhibitor latrunculin A (lat A; Fig. 5, B and C), indicating that the Sla1p patches on the cortex and inside of the cell exhibit actin assembly–dependent turnover.

Previous analysis by electron microscopy and by use of the fluorescent membrane marker FM4-64 revealed abnormal deep membrane invaginations in *sjl1Δ sjl2Δ* cells (Srinivasan et al., 1997; Singer-Kruger et al., 1998; Stefan et al., 2002). To determine if the internal Sla1-GFP patches are present on the abnormal invaginations, we imaged Sla1-GFP and FM4-64 at the same time in *sjl1Δ sjl2Δ* cells. Strikingly, all of the internal Sla1-GFP patches appeared to be associated with the abnormal internal membrane structures labeled by FM4-64 (Fig. 6 A). The internal FM4-64 staining in *sjl1Δ sjl2Δ* cells was probably not the result of endocytosis because no internal FM4-64 signal was observed in wild-type cells at this early time point (Fig. 6 A). In addition, we incubated both wild-type and *sjl1Δ sjl2Δ* cells with Alexa Fluor 594–α-factor (Toshima et al., 2006), which is a cargo for receptor-mediated endocytosis, and imaged both the Alexa Fluor signal and Sla1-GFP immediately after internalization was initiated by shifting cells from ice to room temperature. At this early time, Alexa Fluor labeled the abnormal internal structures that existed in the *sjl1Δ sjl2Δ* cells, but did not label internal structures in wild-type cells. This result strongly suggests that the internal membrane structures are continuous with the plasma membrane (Fig. 6 B). Furthermore, two-color real-time microscopy revealed that during a 2-min video of the *sjl1Δ sjl2Δ* cells, multiple Sla1-GFP patches appear and disappear at different areas of the deep internal structures labeled by FM4-64 (Fig. 7 A and Video 6, available at http://www.jcb.org/cgi/content/full/jcb.200611011/DC1). Similar results were also obtained when we simultaneously imaged GFP-tagged Pdr5 (ATP-binding cassette transporter), which is known to localize at the plasma membrane, and the actin patch marker Abp1-RFP in *sjl1Δ sjl2Δ* cells (Fig. 7 B and Video 7). Multiple Abp1p patches appeared and disappeared on Pdr5-GFP–labeled internal structures (Video 7). The abnormal, deeply invaginated membrane structures in *sjl1Δ sjl2Δ* cells were previously observed and proposed to result from failure of endocytic vesicle fission (Singer-Kruger et al., 1998; Stefan et al., 2002). However, our two-color live-cell imaging analysis indicated that endocytic protein patches continuously assemble and disassemble on these structures, much as they do on the rest of plasma membrane.

Next, to gain insights into PtdIns(4,5)P_2 distribution on the cell cortex and abnormal internal membrane structures, we imaged the only yeast phosphatidylinositol-4-phosphate 5-kinase, Mss4-GFP, and the plasma membrane marker Prd5-RFP, in *sjl1Δ sjl2Δ* cells. Mss4p patches were also observed in the deeply invaginated membrane structures, suggesting PtdIns(4,5)P_2 can be produced on these structures (Fig. 6 C). In addition, we crossed *sla2 ANTH-GFP* into the *sjl1Δ sjl2Δ* background. Although the *sjl1Δ sjl2Δ sla2Δ* triple mutant is inviable (unpublished data), an *sjl1Δ sjl2Δ sla2ANTH-GFP* strain is viable. In *sjl1Δ sjl2Δ sla2ANTH-GFP* cells, Sla2 ANTH-GFP showed patch localization with a lifetime of 76.5 ± 13.2 s, both on the cell cortex and on the abnormal membrane invagination (Fig. 6 D). It is surprising that Sla2 ANTH-GFP in the *sjl1Δ sjl2Δ* strain had a shorter

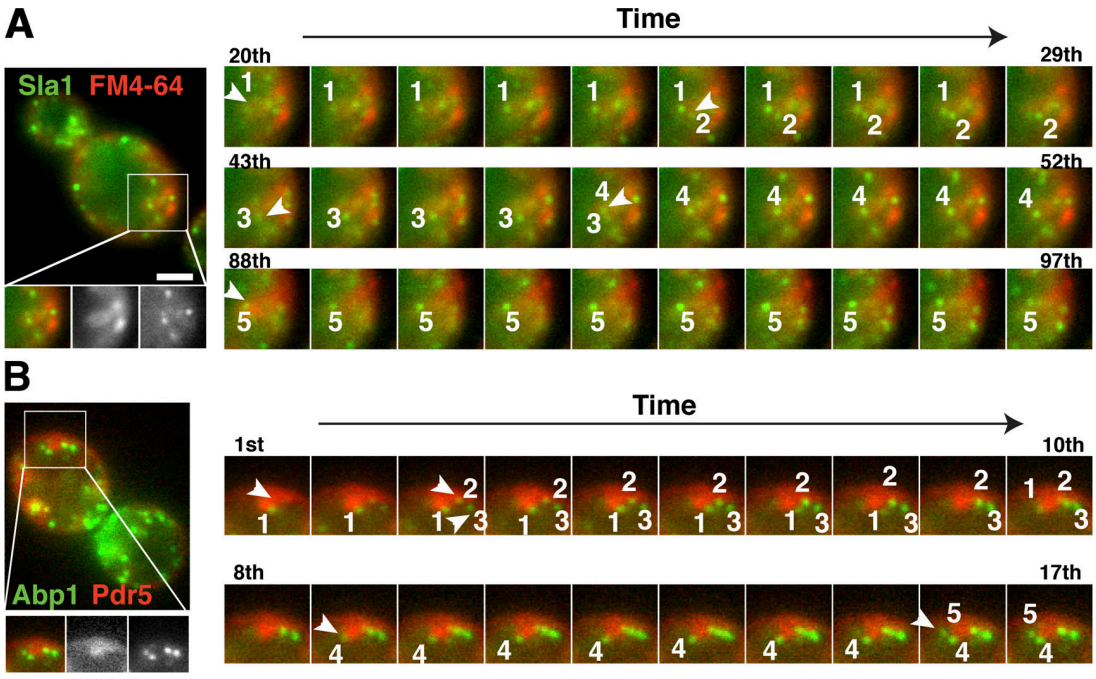

Figure 7. **Sla1 patch dynamics in the abnormal, deep membrane invaginations of *sjl1Δ sjl2Δ* mutants.** (A) FM4-64 labeling over time of *sjl1Δ sjl2Δ* cells expressing Sla1-GFP. Single image from two-color video (left). FM4-64 is red, and Sla1-GFP is green. Selected frames show Sla1 patch dynamics at one deep, abnormal membrane invagination structure over time (right). The time to acquire one image pair was 2.8 s. The numbers in black indicate the frame number of the video. The numbers in white indicate different patches. (B) Two-color imaging of *sjl1Δ sjl2Δ* cells expressing Abp1-GFP and Pdr5-RFP. Selected frames show Abp1 patch dynamics at one deep, abnormal membrane invagination structure over time (right). Time to acquire one image pair was 2.8 s. The numbers in black indicate the frame number of the video and the numbers in white indicate different patches. Bar, 2 μm.

lifetime than in wild-type cells (105 ± 28.7). Perhaps in the *sjl1Δ sjl2Δ sla2ANTH-GFP* strain, failure to carry out productive endocytic events results in premature disassembly of the endocytic machinery. Nevertheless, dynamic assembly of endocytic proteins on the abnormal membrane invaginations provides evidence that endocytic proteins do not recognize membrane compartments by virtue of where the membrane compartment localizes in the cell, but by virtue of the membrane's specific molecular components, including PtdIns(4,5)P_2.

sjl1Δ sjl2Δ cells are defective in functions of multiple endocytic modules

Previously, based on the dynamic behavior of many different proteins during endocytic internalization, we proposed that the yeast endocytic machinery is composed of four protein modules (Kaksonen et al., 2005). To test how failure to properly regulate PtdIns(4,5)P_2 levels affects the behavior of the different endocytic modules, we analyzed the dynamics of proteins representing each module in *sjl1Δ sjl2Δ* mutants.

The coat module consists of proteins that assemble on the plasma membrane and then internalize ~200 nm before disassembling. We analyzed the dynamic behavior of the coat proteins Sla1p, Sla2p, and Ent1p in *sjl1Δ sjl2Δ* cells (Fig. 8, A and C; and Videos 8–10, available at http://www.jcb.org/cgi/content/full/jcb.200611011/DC1). Strikingly, kymographs of the patches revealed that all of these proteins still undergo inward movement, indicating that invagination occurs in this mutant (Fig. 8 A). These results are consistent with the fact that Sjl2p is recruited

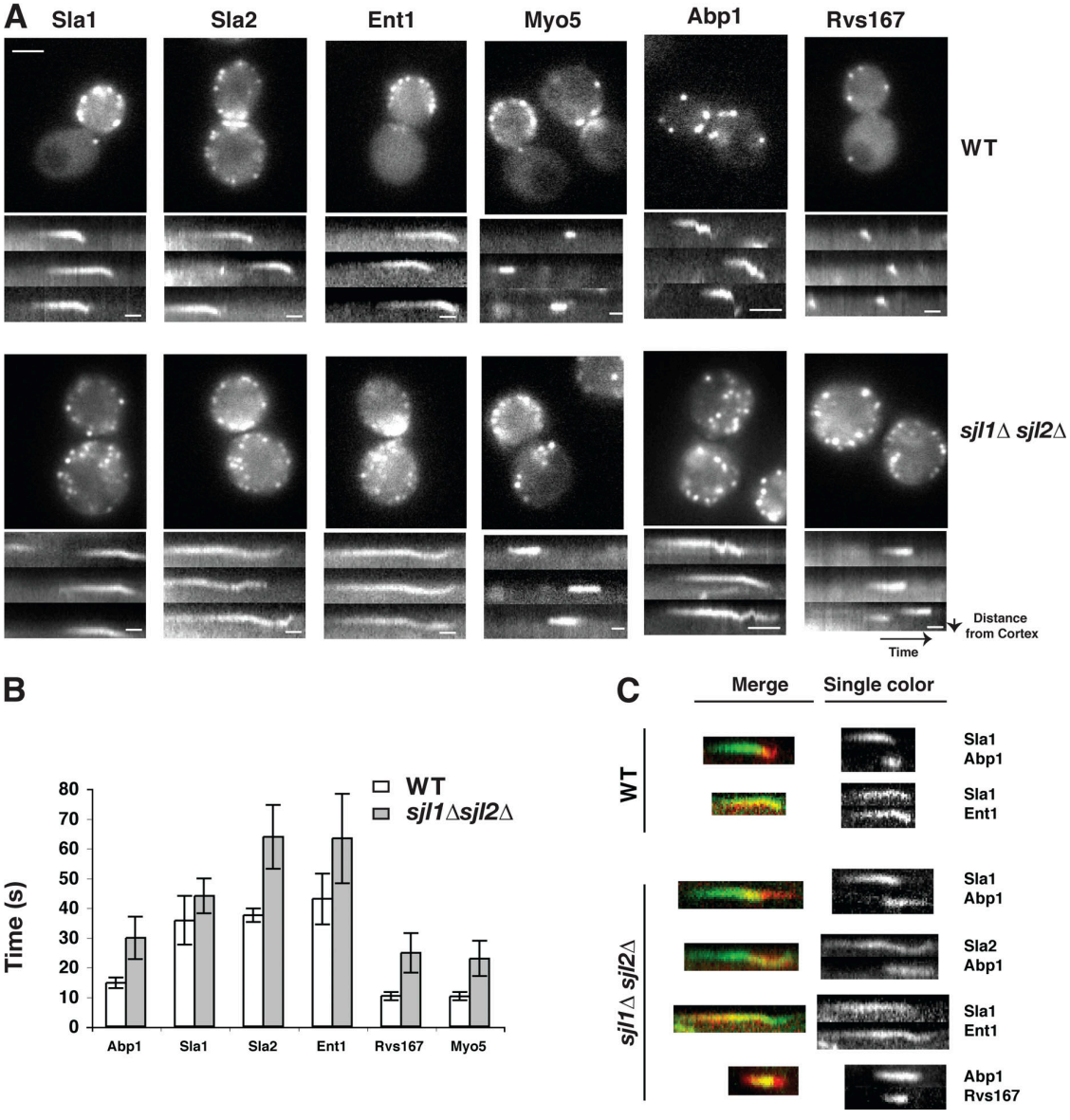

Figure 8. **Different endocytic modules have distinct defects in *sjl1Δ sjl2Δ* mutant.** (A) Single frames from videos of wild-type or *sjl1Δ sjl2Δ* cells expressing different GFP-tagged endocytic proteins (first and third column). Bars, 2 μm. Kymographs of single patches from videos of cells expressing the indicated GFP-tagged protein (second and fourth columns). Scale bars for kymographs are 10 s. (B) Lifetimes for different patch proteins ± standard deviation. n = 30 patches for each strain. White bars indicate wild-type cells and gray bars indicate *sjl1Δ sjl2Δ* cells. (C) Kymographs of single patches from two-color videos of cells expressing the indicated GFP- and RFP-tagged proteins.

to endocytic sites only after the slow Sla1p movement starts in wild-type cells (Fig. 4 D). However, after the inward movement, Sla2p and Ent1p persisted much longer than Sla1p in *sjl1Δ sjl2Δ* cells (Fig. 8, A and B; and Videos 8 and 9). This may be because both Sla2p and Ent1p contain PtdIns(4,5)P_2 binding domains, whereas Sla1p does not (Aguilar et al., 2003; Sun et al., 2005). Thus, because PtdIns(4,5)P_2 turnover is defective in *sjl1Δ sjl2Δ* cells, Sla2p and Ent1p disassembly are significantly delayed. Previous studies suggested that disassembly of the Sla1p–Pan1p–End3p complex is regulated by phosphorylation activity of the related protein kinases Ark1p and Prk1p (Cope et al., 1999; Zeng and Cai, 1999; Sekiya-Kawasaki et al., 2003). Together, these data suggest that there may be at least two kinds of mechanisms that regulate endocytic coat disassembly. One is based on protein phosphorylation by Ark1p and Prk1p, and the other is based on PtdIns(4,5)P_2 hydrolysis by Sjl2p.

The myosin–WASP module nucleates actin polymerization and, rather than getting internalized, remains at the cell cortex during endocytosis (Kaksonen et al., 2003; Jonsdottir and Li, 2004; Sun et al., 2006). Myo5p, which belongs to the type I myosin family, has a lifetime of 22.8 ± 5.9 s in *sjl1Δ sjl2Δ* cells, which is about double its lifetime in wild-type cells (Fig. 8, A and B, and Video 8; Sun et al., 2006). One mammalian type I myosin, Myo1c, has been shown to bind tightly and specifically to PtdIns(4,5)P_2, as well as to inositol 1,4,5-trisphosphate (Hokanson and Ostap, 2006). More recently, Myo1c has been shown to bind phosphoinositides through a putative pleckstrin homology (PH) domain (Hokanson et al., 2006). This putative PH domain is also conserved in Myo5p. Thus, the delay in Myo5p disassembly may be a direct effect of the PtdIns(4,5)P_2 turnover defect.

Like the myosin–WASP module, actin and several other proteins of the actin-associated protein module are absolutely essential for yeast endocytosis. We used Abp1-GFP as a marker to monitor actin behavior. In *sjl1Δ sjl2Δ* mutants, actin assembly was slightly delayed, which is consistent with the observation that the endocytic coat module undergoes slow inward movement that is likely correlated with membrane invagination (Fig. 9). However, Abp1p showed a significantly longer patch lifetime ($P < 0.01$) in *sjl1Δ sjl2Δ* cells than in wild-type cells (Fig. 8, A and B, Fig. 9, and Video 8). Previously, we proposed that actin assembly promotes endocytic coat invagination and that actin disassembly may occur upon endocytic vesicle release (Kaksonen et al., 2003). Together, our results indicate that PtdIns(4,5)P_2 levels are important for actin regulation at endocytic sites.

The scission module consists of the yeast amphiphysin homologues Rvs161p and Rvs167p, which can heterodimerize. In yeast, Rvs161p and Rvs167p arrive at endocytic sites after actin polymerization starts. After briefly remaining stationary in a patch, Rvs161p and Rvs167p move rapidly inward ~100 nm. This rapid inward movement was proposed to correspond to vesicle scission (Kaksonen et al., 2005). In *sjl1Δ sjl2Δ* cells, Rvs167p still appears after Abp1p appears, but it remains at the sites 2–3 times longer than it does in wild-type cells (Fig. 8, B and C, and Video 8). *sjl1Δ sjl2Δ* cells exhibit a severe defect in both receptor-mediated and fluid-phase endocytosis, suggesting that vesicle scission may not occur in this mutant. Importantly, Rvs167p does not make inward movements in *sjl1Δ sjl2Δ* cells, supporting this idea. Thus, these results suggest that PtdIns(4,5)P_2 turnover is important for Rvs161p/167p function in endocytic scission.

Discussion

In this study, two GFP-tagged protein probes, Sla2 ANTH-GFP and Sjl2-3GFP, were used to quantitatively analyze PtdIns(4,5)P_2

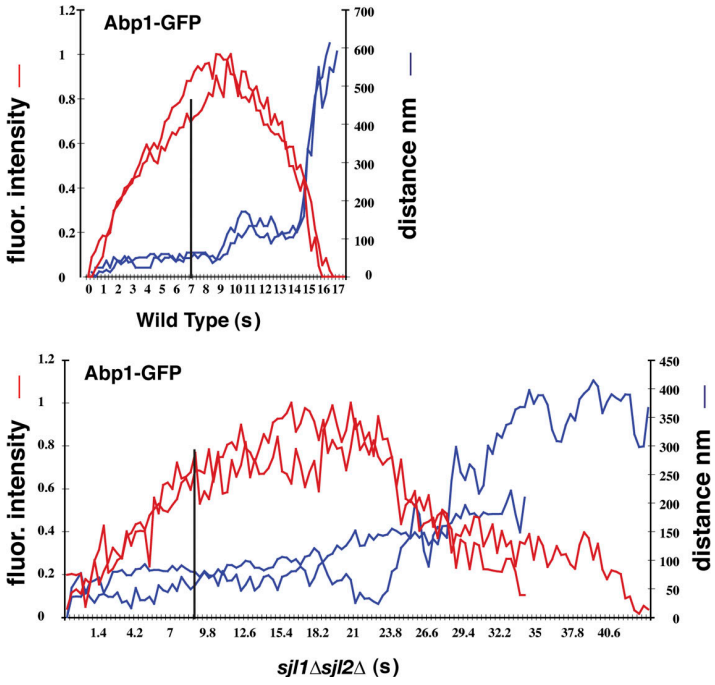

Figure 9. **Dynamic Abp1 behavior in *sjl1Δ sjl2Δ* cells.** Quantitation of fluorescence intensity and distance from the site of patch formation for Abp1-GFP–labeled patches as a function of time in wild-type cells and *sjl1Δ sjl2Δ* cells. Each curve represents data from one patch. Fluorescence intensity over time was corrected for photobleaching. The vertical black line indicates the time point when Abp1-GFP reaches 80% of the peak intensity.

dynamics at endocytic sites in budding yeast. We also imaged dynamics of endocytic module proteins in a synaptojanin mutant to investigate the functions of PtdIns(4,5)P_2 turnover during endocytosis. The results revealed an intimate link between PtdIns(4,5)P_2 dynamic regulation and multiple stages during the endocytic internalization.

Sla2 ANTH-GFP is a specific marker for PtdIns(4,5)P_2 at endocytic sites

We expressed Sla2 ANTH-GFP at endogenous levels in budding yeast in place of wild-type Sla2p, and found that endocytosis was partially functional in this strain. It is not clear whether Sla2 ANTH-GFP has protein-binding partners. However, Sla2 ANTH-GFP, but not Sla2 4K-A ANTH-GFP, which is specifically defective in PtdIns(4,5)P_2 binding (Sun et al., 2005), localized to endocytic sites, indicating that localization of Sla2 ANTH-GFP at endocytic sites is dependent on its PtdIns(4,5)P_2 interaction. Importantly, Sla2 ANTH-GFP localization to endocytic sites lends support to the hypothesis that these sites may correspond to PtdIns(4,5)P_2-enriched microdomains (Carlton and Cullen, 2005). Furthermore, Sla2 ANTH-GFP showed indistinguishable behavior to endocytic coat proteins such as Sla1-mCherry, establishing a tight link between PtdIns(4,5)P_2 and the presence of endocytic coat proteins. These results implicate PtdIns(4,5)P_2 enrichment and turnover in endocytic coat formation and disassembly, respectively.

Uniform distribution of Mss4-GFP patches on the plasma membrane suggested that PtdIns(4,5)P_2 may not be selectively synthesized at sites of endocytosis. Sla2 ANTH-mCherry accumulated in endocytic patches shortly after Clc1-GFP appeared in the patches, suggesting that PtdIns(4,5)P_2 enrichment at endocytic sites occurs after the recruitment of cargo molecules has begun. Previously, it was shown that endocytic-site assembly is 50–75% reduced in *clc1Δ* cells (Kaksonen et al., 2005). We also found that Sla2 ANTH-GFP patches form on the plasma membrane at a similarly reduced rate in *clc1Δ* cells (unpublished data). These results support the possibility that PtdIns(4,5)P_2 enrichment occurs concomitantly, and possibly synergistically, with endocytic coat assembly. Unlike Sla2 ANTH-GFP, which shows the patchlike localization that characterizes endocytic proteins, overexpressed GFP-2xPLCδ-PH from rat labeled the yeast plasma membrane uniformly (Stefan et al., 2002). High expression of GFP-2xPLCδ-PH may have affected the ability to detect local differences in PtdIns(4,5)P_2 levels on the plasma membrane. Alternately, high expression of GFP-2xPLCδ-PH may have sequestered PtdIns(4,5)P_2 and prevented PtdIns(4,5)P_2 recruitment to endocytic patches. Finally, because both ANTH domains and PLCδ-PH bind to PtdIns(4,5)P_2 specifically in vitro (Lemmon et al., 1995; Sun et al., 2005), the different patterns of membrane localization in vivo might reflect differences in PtdIns(4,5)P_2 binding affinity, or different protein-binding partners for ANTH and PLCδ-PH domains, which may affect their localization and functions. Further studies are needed to determine the mechanism of PtdIns(4,5)P_2 enrichment at endocytic sites.

PtdIns(4,5)P_2 dynamics during endocytic internalization

Quantitative, high time resolution, live-cell imaging of Sjl2-3GFP expressed at endogenous levels allowed us to precisely analyze its dynamics relative to key events during endocytic internalization. Sjl2p only accumulated at endocytic sites after bulk actin assembly and endocytic coat assembly reached their maximum levels, suggesting that PtdIns(4,5)P_2 hydrolysis may attenuate coat and actin assembly. These results are consistent with the possibility that PtdIns(4,5)P_2 plays roles in recruitment of the endocytic machinery to the plasma membrane and in promoting actin polymerization. Sjl2p levels were maximal when coat disassembly and actin disassembly were occurring, which is in agreement with a role for a decrease in PtdIns(4,5)P_2 levels in driving these disassembly processes. Additionally, the time period during which Sjl2p levels are maximal also coincides with the time when the Abp1p/Sjl2p fast movement occurs, suggesting that the decrease in PtdIns(4,5)P_2 levels occurs close to the time of vesicle scission. This observation is consistent with the proposal that local lipid composition changes may result in a phase separation that will promote vesicle scission (Roux et al., 2005; Liu et al., 2006). Finally, the Sjl2p dynamics provide further support for the conclusion that Sla2 ANTH-GFP is a valid probe for PtdIns(4,5)P_2 because recruitment of the former protein to endocytic sites precedes a decrease in levels of the latter protein.

Abnormal deep membrane invaginations in *sjl1Δ sjl2Δ* cells with elevated PtdIns(4,5)P_2 levels continuously assemble abortive endocytic sites

Results from our two-color live-cell imaging analysis of endocytic protein dynamics in *sjl1Δ sjl2Δ* cells have caused us to reconsider a previously posited model for how abnormal deep plasma membrane invaginations are formed in this mutant (Singer-Kruger et al., 1998; Stefan et al., 2005), and provide insights into the nature of the signal that promotes endocytic site assembly.

It had previously been proposed that these deep membrane invaginations might represent formation of a single endocytic site, followed by a failure of vesicle scission (Singer-Kruger et al., 1998; Stefan et al., 2005). However, upon observing endocytic protein dynamics and plasma membrane simultaneously in *sjl1Δ sjl2Δ* cells, we found that multiple endocytic sites form and disappear on the deep plasma membrane invaginations. Our data also suggest that these abnormal invaginations exhibit PtdIns(4,5)P_2 foci similar to those on the plasma membrane. Thus, this mutant lends further support to the hypothesis that the endocytic site formation is not determined by where the membrane compartment localizes in the cell, but may be determined by the membrane's specific molecular components, including PtdIns(4,5)P_2 (Honing et al., 2005).

How do these deep membrane invaginations form in *sjl1Δ sjl2Δ* mutants? Previous studies showed that inhibiting actin polymerization before impairing synaptojanin function prevents formation of the deep membrane invaginations, suggesting that actin assembly is important for formation of the abnormal

membrane structures (Stefan et al., 2005). Consistently in our studies, the abnormal membrane structures were not observed in *vrp1Δ sjl1Δ sjl2Δ* mutants (unpublished data). Vrp1 appears before actin/Sjl2p and formation of endocytic invaginations is completely defective in *vrp1Δ* mutants (Sun et al., 2006). We speculate that the large abnormal membrane invaginations are the result of hyperactive initiation of endocytic sites, with continuous abortive endocytic events occurring one on top of the other. The abortive endocytic events are presumably initiated as a result of elevated PtdIns(4,5)P_2 levels, and because of a lack of PtdIns(4,5)P_2 turnover, which may result in a failure to appropriately perform individual endocytic events, including vesicle scission.

PtdIns(4,5)P_2 importance for dynamic functions of different endocytic modules

Failure to properly regulate PtdIns(4,5)P_2 in *sjl1Δ sjl2Δ* mutants caused different defects in dynamics of the endocytic coat proteins Sla1p and Sla2p, suggesting the existence of distinct uncoating mechanisms. Interestingly, recruitment of Ark1p, Prk1p, and Sjl2p, which are all negative regulators of the endocytic machinery, to endocytic sites is dependent on Abp1p/F-actin (Cope et al., 1999; Fazi et al., 2002; Sekiya-Kawasaki et al., 2003; Stefan et al., 2005). Moreover, two-color real-time analysis revealed that the protein kinase Prk1p also shows very similar dynamic behavior to the lipid phosphatase Sjl2p (unpublished data by Lee L., Sekiya-Kawasaki M., and D.G.D), suggesting that the two systems may work concurrently. This dual system may provide an efficient and reliable way to promote uncoating of endocytic membranes, which contain many different proteins with complicated protein–protein and/or protein–lipid interactions.

Our results also demonstrate a significant actin disassembly delay in *sjl1Δ sjl2Δ* mutants. There are several factors that may contribute to such a delay. First, Myo5p, which is a major Arp2/3 activator during endocytic internalization (Sun et al., 2006), persists at endocytic sites much longer in the mutant than in wild-type cells. Second, Sla2p, Ent1p, and perhaps other PtdIns(4,5)P_2-binding proteins may play regulatory roles in actin organization. The delay in coat disassembly may therefore contribute to actin disassembly defects. Finally, previous data suggest that actin-binding proteins, including cofilin and capping protein, which function to promote actin filament depolymerization, and to attenuate polymerization, respectively, are negatively regulated by PtdIns(4,5)P_2 (Yin and Janmey, 2003). We speculate that a defect in PtdIns(4,5)P_2 turnover may impair actin disassembly by inhibiting these actin-binding proteins.

Mutants defective in synaptojanin function have been extensively examined in many different organisms (Srinivasan et al., 1997; Singer-Kruger et al., 1998; Stolz et al., 1998; Cremona et al., 1999; Gad et al., 2000; Harris et al., 2000; Verstreken et al., 2003; Stefan et al., 2005). Although electron microscopy and immunostaining studies have been very useful for characterizing the terminal morphological membrane defects in these mutants, the temporal resolution that live-cell imaging affords provided us with a very sensitive method with which to analyze defects in specific endocytic steps that generate the terminal phenotype. We found that in *sjl1Δ sjl2Δ* cells, proteins from each of the four different endocytic modules previously identified get recruited to the plasma membrane in the appropriate order, and they form endocytic sites (Fig. 8 C and Videos 8 and 9). However, distinct defects in the behavior and functions of different endocytic modules in the aforementioned *sjl1Δ sjl2Δ* cells allowed us to better understand the function of PtdIns(4,5)P_2 turnover at the different stages of endocytic internalization.

Clathrin-mediated endocytosis in yeast and mammalian cells is far more similar than had previously been appreciated. Many components of the mammalian endocytic machinery, including Hip1R and synaptojanin, share homology to yeast endocytic proteins (Sla2p and Sjl1p/Sjl2p, respectively). Thus, we anticipate that the dynamics and the functions of PtdIns(4,5)P_2 revealed in this study are relevant in more complex cells.

Materials and methods

Plasmids and strains

Yeast strains used in this study are listed in Table S1 (available at http://www.jcb.org/cgi/content/full/jcb.200609014/DC1). C-terminal GFP and RFP tags were integrated by homologous recombination, as previously described (Sun et al., 2006). We cloned *SJL2-3GFP* using PBS-3xGFP–His vector, which was modified from the pBS-3xGFP–Trp vector (W.-L. Lee, University of Massachusetts, Amherst, MA; Lee et al., 2003). The resulting plasmids contain a fragment encoding the C terminus of Sjl2p fused in frame to a five Ala linker and triple GFP. Wild-type haploid cells (DDY 904) were transformed with this vector linearized by an appropriate restriction enzyme in the middle of the *SJL2* sequence. Stable His^+ transformants were selected and screened for proper targeting by PCR.

α-factor uptake assay

^{35}S-labeled α-factor was prepared as described in Howard et al. (2002). The α-factor uptake assay was performed at 25°C, based on a continuous incubation protocol (Sekiya-Kawasaki et al., 2003). Cells were grown in YPD, harvested by centrifugation, and resuspended in internalization media (YPD media with 0.5% casamino acids and 1% BSA). At the indicated time points, aliquots were withdrawn and diluted in ice-cold buffer at pH 6.0 (total α-factor) or pH 1.1 (internalized α-factor). The samples were then filtered and radioactivity was measured in a scintillation counter. The results were expressed as the ratio of pH 1.1 cpm/pH 6.0 cpm for each time point to represent the percentage of internalization.

Fluorescence microscopy

FM4-64 staining was done in a flow chamber, as previously described (Sekiya-Kawasaki et al., 2003). Imaging was performed immediately after the addition of the dye, which was used at a concentration of 8 μM in SD-based media (Sekiya-Kawasaki et al., 2003). Alexa Fluor 594–α-factor imaging was done as previously described (Toshima et al., 2006). One-color live-cell imaging and two-color live-cell imaging were performed as previously described (Sun et al., 2006). Cells were attached to concanavalin A–coated coverslips, which were sealed to slides with vacuum grease (Dow Corning). All imaging studies were performed at ∼25°C using a microscope (IX81; Olympus) equipped with 100×/NA 1.4 objectives and cameras (Orca II; Hamamatsu). Image analysis was performed with ImageJ (National Institutes of Health; http://rsb.info.nih.gov/ij/; Kaksonen et al., 2003).

Online supplemental material

Fig. S1 shows results of experiments demonstrating that Mss4-GFP, Sjl1-GFP, and Sjl2-3GFP are functional in vivo, and results of localization of these GFP-tagged proteins. Video 1 includes real-time videos of Sla2 ANTH-GFP and Sla2 4K-A ANTH-GFP dynamics in vivo. Video 2 is a two-color real-time video of Sla2 ANTH-GFP and Sla1-mCherry (provided by C. Toret, University of California, Berkeley, Berkeley, CA) dynamics in vivo. Video 3 is a two-color real-time video of Sla2 ANTH-GFP and Abp1-mRFP dynamics in vivo. Video 4 includes real-time videos of Sjl2-GFP or Sjl2-3GFP dynamics in vivo. Video 5 is a two-color real-time video of Sjl1-3GFP

and Abp1-mRFP dynamics in vivo. Video 6 is a two-color real-time video of Sla1-GFP and FM4-64 in *sjl1Δ sjl2Δ* cells. Video 7 is a two-color real-time video of Abp1-GFP and Pdr5-RFP in *sjl1Δ sjl2Δ* cells. Video 8 includes real-time videos of various proteins tagged with GFP in wild-type cells or in *sjl1Δ sjl2Δ* cells. Video 9 includes two-color real-time videos of various proteins tagged with GFP or RFP in wild-type cells or in *sjl1Δ sjl2Δ* cells. Video 10 includes two-color real-time videos of Ent1-GFP and Sla1-mCherry in wild-type cells or in *sjl1Δ sjl2Δ* cells. Table S1 is a list of yeast strains used in this study. The online version of this article is available at http://www.jcb.org/cgi/content/full/jcb.200611011/DC1.

We thank Wei-Lih Lee for providing the pBS-3xGFP–Trp vector. We also thank Christopher Toret for providing the Sla1-mCherry strain. We thank Voytek Okreglak and Christopher Toret for preparing the ^{35}S-labeled α-factor. We thank the members of the Drubin laboratory for helpful discussions, and Brian Young, Voytek Okreglak, Jonathan Wong, and Barbara Pauly for critical reading of the manuscript.

This work was supported by National Institutes of Health grants GM42759 and GM 50399 to D.G. Drubin.

Submitted: 3 November 2006
Accepted: 21 March 2007

References

Aguilar, R.C., H.A. Watson, and B. Wendland. 2003. The yeast Epsin Ent1 is recruited to membranes through multiple independent interactions. *J. Biol. Chem.* 278:10737–10743.

Bairstow, S.F., K. Ling, X. Su, A.J. Firestone, C. Carbonara, and R.A. Anderson. 2006. Type Igamma661 phosphatidylinositol phosphate kinase directly interacts with AP2 and regulates endocytosis. *J. Biol. Chem.* 281:20632–20642.

Carlton, J.G., and P.J. Cullen. 2005. Coincidence detection in phosphoinositide signaling. *Trends Cell Biol.* 15:540–547.

Cope, M.J., S. Yang, C. Shang, and D.G. Drubin. 1999. Novel protein kinases Ark1p and Prk1p associate with and regulate the cortical actin cytoskeleton in budding yeast. *J. Cell Biol.* 144:1203–1218.

Cremona, O., G. Di Paolo, M.R. Wenk, A. Luthi, W.T. Kim, K. Takei, L. Daniell, Y. Nemoto, S.B. Shears, R.A. Flavell, et al. 1999. Essential role of phosphoinositide metabolism in synaptic vesicle recycling. *Cell*. 99:179–188.

Desrivieres, S., F.T. Cooke, P.J. Parker, and M.N. Hall. 1998. MSS4, a phosphatidylinositol-4-phosphate 5-kinase required for organization of the actin cytoskeleton in *Saccharomyces cerevisiae*. *J. Biol. Chem.* 273:15787–15793.

Desrivieres, S., F.T. Cooke, H. Morales-Johansson, P.J. Parker, and M.N. Hall. 2002. Calmodulin controls organization of the actin cytoskeleton via regulation of phosphatidylinositol (4,5)-bisphosphate synthesis in *Saccharomyces cerevisiae*. *Biochem. J.* 366:945–951.

Di Paolo, G., H.S. Moskowitz, K. Gipson, M.R. Wenk, S. Voronov, M. Obayashi, R. Flavell, R.M. Fitzsimonds, T.A. Ryan, and P. De Camilli. 2004. Impaired PtdIns(4,5)P2 synthesis in nerve terminals produces defects in synaptic vesicle trafficking. *Nature*. 431:415–422.

Fazi, B., M.J. Cope, A. Douangamath, S. Ferracuti, K. Schirwitz, A. Zucconi, D.G. Drubin, M. Wilmanns, G. Cesareni, and L. Castagnoli. 2002. Unusual binding properties of the SH3 domain of the yeast actin-binding protein Abp1: structural and functional analysis. *J. Biol. Chem.* 277:5290–5298.

Ford, M.G., B.M. Pearse, M.K. Higgins, Y. Vallis, D.J. Owen, A. Gibson, C.R. Hopkins, P.R. Evans, and H.T. McMahon. 2001. Simultaneous binding of PtdIns(4,5)P2 and clathrin by AP180 in the nucleation of clathrin lattices on membranes. *Science*. 291:1051–1055.

Friesen, H., C. Humphries, Y. Ho, O. Schub, K. Colwill, and B. Andrews. 2006. Characterization of the yeast amphiphysins Rvs161p and Rvs167p reveals roles for the Rvs heterodimer in vivo. *Mol. Biol. Cell*. 17:1306–1321.

Gad, H., N. Ringstad, P. Low, O. Kjaerulff, J. Gustafsson, M. Wenk, G. Di Paolo, Y. Nemoto, J. Crun, M.H. Ellisman, et al. 2000. Fission and uncoating of synaptic clathrin-coated vesicles are perturbed by disruption of interactions with the SH3 domain of endophilin. *Neuron*. 27:301–312.

Gaidarov, I., and J.H. Keen. 1999. Phosphoinositide-AP-2 interactions required for targeting to plasma membrane clathrin-coated pits. *J. Cell Biol.* 146:755–764.

Gourlay, C.W., H. Dewar, D.T. Warren, R. Costa, N. Satish, and K.R. Ayscough. 2003. An interaction between Sla1p and Sla2p plays a role in regulating actin dynamics and endocytosis in budding yeast. *J. Cell Sci.* 116:2551–2564.

Haffner, C., K. Takei, H. Chen, N. Ringstad, A. Hudson, M.H. Butler, A.E. Salcini, P.P. Di Fiore, and P. De Camilli. 1997. Synaptojanin 1: localization on coated endocytic intermediates in nerve terminals and interaction of its 170 kDa isoform with Eps15. *FEBS Lett.* 419:175–180.

Harris, T.W., E. Hartwieg, H.R. Horvitz, and E.M. Jorgensen. 2000. Mutations in synaptojanin disrupt synaptic vesicle recycling. *J. Cell Biol.* 150:589–600.

Henry, K.R., K. D'Hondt, J. Chang, T. Newpher, K. Huang, R.T. Hudson, H. Riezman, and S.K. Lemmon. 2002. Scd5p and clathrin function are important for cortical actin organization, endocytosis, and localization of sla2p in yeast. *Mol. Biol. Cell*. 13:2607–2625.

Hokanson, D.E., and E.M. Ostap. 2006. Myo1c binds tightly and specifically to phosphatidylinositol 4,5-bisphosphate and inositol 1,4,5-trisphosphate. *Proc. Natl. Acad. Sci. USA*. 103:3118–3123.

Hokanson, D.E., J.M. Laakso, T. Lin, D. Sept, and E.M. Ostap. 2006. Myo1c binds phosphoinositides through a putative pleckstrin homology domain. *Mol. Biol. Cell*. 17:4856–4865.

Homma, K., S. Terui, M. Minemura, H. Qadota, Y. Anraku, Y. Kanaho, and Y. Ohya. 1998. Phosphatidylinositol-4-phosphate 5-kinase localized on the plasma membrane is essential for yeast cell morphogenesis. *J. Biol. Chem.* 273:15779–15786.

Honing, S., D. Ricotta, M. Krauss, K. Spate, B. Spolaore, A. Motley, M. Robinson, C. Robinson, V. Haucke, and D.J. Owen. 2005. Phosphatidylinositol-(4,5)-bisphosphate regulates sorting signal recognition by the clathrin-associated adaptor complex AP2. *Mol. Cell*. 18:519–531.

Howard, J.P., J.L. Hutton, J.M. Olson, and G.S. Payne. 2002. Sla1p serves as the targeting signal recognition factor for NPFX(1,2)D-mediated endocytosis. *J. Cell Biol.* 157:315–326.

Itoh, T., S. Koshiba, T. Kigawa, A. Kikuchi, S. Yokoyama, and T. Takenawa. 2001. Role of the ENTH domain in phosphatidylinositol-4,5-bisphosphate binding and endocytosis. *Science*. 291:1047–1051.

Jonsdottir, G.A., and R. Li. 2004. Dynamics of yeast Myosin I: evidence for a possible role in scission of endocytic vesicles. *Curr. Biol.* 14:1604–1609.

Jost, M., F. Simpson, J.M. Kavran, M.A. Lemmon, and S.L. Schmid. 1998. Phosphatidylinositol-4,5-bisphosphate is required for endocytic coated vesicle formation. *Curr. Biol.* 8:1399–1402.

Kaksonen, M., Y. Sun, and D.G. Drubin. 2003. A pathway for association of receptors, adaptors, and actin during endocytic internalization. *Cell*. 115:475–487.

Kaksonen, M., C.P. Toret, and D.G. Drubin. 2005. A modular design for the clathrin- and actin-mediated endocytosis machinery. *Cell*. 123:305–320.

Lee, W.L., J.R. Oberle, and J.A. Cooper. 2003. The role of the lissencephaly protein Pac1 during nuclear migration in budding yeast. *J. Cell Biol.* 160:355–364.

Lemmon, M.A., K.M. Ferguson, R. O'Brien, P.B. Sigler, and J. Schlessinger. 1995. Specific and high-affinity binding of inositol phosphates to an isolated pleckstrin homology domain. *Proc. Natl. Acad. Sci. USA*. 92:10472–10476.

Liu, J., M. Kaksonen, D.G. Drubin, and G. Oster. 2006. Endocytic vesicle scission by lipid phase boundary forces. *Proc. Natl. Acad. Sci. USA*. 103:10277–10282.

McCann, R.O., and S.W. Craig. 1997. The I/LWEQ module: a conserved sequence that signifies F-actin binding in functionally diverse proteins from yeast to mammals. *Proc. Natl. Acad. Sci. USA*. 94:5679–5684.

McPherson, P.S., E.P. Garcia, V.I. Slepnev, C. David, X. Zhang, D. Grabs, W.S. Sossin, R. Bauerfeind, Y. Nemoto, and P. De Camilli. 1996. A presynaptic inositol-5-phosphatase. *Nature*. 379:353–357.

Merrifield, C.J. 2004. Seeing is believing: imaging actin dynamics at single sites of endocytosis. *Trends Cell Biol.* 14:352–358.

Padron, D., Y.J. Wang, M. Yamamoto, H. Yin, and M.G. Roth. 2003. Phosphatidylinositol phosphate 5-kinase Iβ recruits AP-2 to the plasma membrane and regulates rates of constitutive endocytosis. *J. Cell Biol.* 162:693–701.

Roux, A., D. Cuvelier, P. Nassoy, J. Prost, P. Bassereau, and B. Goud. 2005. Role of curvature and phase transition in lipid sorting and fission of membrane tubules. *EMBO J.* 24:1537–1545.

Sekiya-Kawasaki, M., A.C. Groen, M.J. Cope, M. Kaksonen, H.A. Watson, C. Zhang, K.M. Shokat, B. Wendland, K.L. McDonald, J.M. McCaffery, and D.G. Drubin. 2003. Dynamic phosphoregulation of the cortical actin cytoskeleton and endocytic machinery revealed by real-time chemical genetic analysis. *J. Cell Biol.* 162:765–772.

Singer-Kruger, B., Y. Nemoto, L. Daniell, S. Ferro-Novick, and P. De Camilli. 1998. Synaptojanin family members are implicated in endocytic membrane traffic in yeast. *J. Cell Sci.* 111:3347–3356.

Srinivasan, S., M. Seaman, Y. Nemoto, L. Daniell, S.F. Suchy, S. Emr, P. De Camilli, and R. Nussbaum. 1997. Disruption of three phosphatidylinositol-polyphosphate 5-phosphatase genes from *Saccharomyces cerevisiae*

results in pleiotropic abnormalities of vacuole morphology, cell shape, and osmohomeostasis. *Eur. J. Cell Biol.* 74:350–360.

Stefan, C.J., A. Audhya, and S.D. Emr. 2002. The yeast synaptojanin-like proteins control the cellular distribution of phosphatidylinositol (4,5)-bisphosphate. *Mol. Biol. Cell*. 13:542–557.

Stefan, C.J., S.M. Padilla, A. Audhya, and S.D. Emr. 2005. The phosphoinositide phosphatase Sjl2 is recruited to cortical actin patches in the control of vesicle formation and fission during endocytosis. *Mol. Cell. Biol.* 25:2910–2923.

Stolz, L.E., C.V. Huynh, J. Thorner, and J.D. York. 1998. Identification and characterization of an essential family of inositol polyphosphate 5-phosphatases (INP51, INP52 and INP53 gene products) in the yeast *Saccharomyces cerevisiae*. *Genetics*. 148:1715–1729.

Sun, Y., M. Kaksonen, D.T. Madden, R. Schekman, and D.G. Drubin. 2005. Interaction of Sla2p's ANTH domain with PtdIns(4,5)P2 is important for actin-dependent endocytic internalization. *Mol. Biol. Cell*. 16:717–730.

Sun, Y., A.C. Martin, and D.G. Drubin. 2006. Endocytic internalization in budding yeast requires coordinated actin nucleation and myosin motor activity. *Dev. Cell*. 11:33–46.

Takei, K., V.I. Slepnev, V. Haucke, and P. De Camilli. 1999. Functional partnership between amphiphysin and dynamin in clathrin-mediated endocytosis. *Nat. Cell Biol.* 1:33–39.

Toshima, J.Y., J. Toshima, M. Kaksonen, A.C. Martin, D.S. King, and D.G. Drubin. 2006. Spatial dynamics of receptor-mediated endocytic trafficking in budding yeast revealed by using fluorescent alpha-factor derivatives. *Proc. Natl. Acad. Sci. USA*. 103:5793–5798.

Vallis, Y., P. Wigge, B. Marks, P.R. Evans, and H.T. McMahon. 1999. Importance of the pleckstrin homology domain of dynamin in clathrin-mediated endocytosis. *Curr. Biol.* 9:257–260.

Verstreken, P., T.W. Koh, K.L. Schulze, R.G. Zhai, P.R. Hiesinger, Y. Zhou, S.Q. Mehta, Y. Cao, J. Roos, and H.J. Bellen. 2003. Synaptojanin is recruited by endophilin to promote synaptic vesicle uncoating. *Neuron*. 40:733–748.

Vida, T.A., and S.D. Emr. 1995. A new vital stain for visualizing vacuolar membrane dynamics and endocytosis in yeast. *J. Cell Biol.* 128:779–792.

Wesp, A., L. Hicke, J. Palecek, R. Lombardi, T. Aust, A.L. Munn, and H. Riezman. 1997. End4p/Sla2p interacts with actin-associated proteins for endocytosis in *Saccharomyces cerevisiae*. *Mol. Biol. Cell*. 8:2291–2306.

Yin, H.L., and P.A. Janmey. 2003. Phosphoinositide regulation of the actin cytoskeleton. *Annu. Rev. Physiol.* 65:761–789.

Zeng, G., and M. Cai. 1999. Regulation of the actin cytoskeleton organization in yeast by a novel serine/threonine kinase Prk1p. *J. Cell Biol.* 144:71–82.